

Equivalent modelling strategy for a clinched joint using a simple calibration method

Andreas Breda^a, Sam Coppieters^a, Dimitri Debruyne^a

^a*Department of Materials Engineering, KU Leuven (Technology Campus Gent), Gebroeders De Smetstraat 1, Gent 9000, Belgium*

Abstract

Clinching is a mechanical joining technique that involves severe local plastic deformation of two or more metal sheet parts resulting in a permanent mechanical interlock. Today, it is a reliable joining technique used in heating, ventilation and air conditioning (HVAC), automotive and general steel constructions whilst still gaining interest. As it is not computationally feasible to include detailed sub models of these type of joints in FE simulations of clinched assemblies during the design stage, this paper proposes a simple methodology to represent these connections with simplified elements. The key point of the method is the use of uncoupled plastic behaviour to model the joint plastic properties. In order to calibrate the parameters governing the equivalent model, a simple shear lap and pull-out reference test of a single clinched joint was used. The presented methodology is validated using a modified Arcan test of a single joint, which enables to exert a combination of shear and pull-out loads. Finally, a peel test is conducted to study the influence of bending moments on the behaviour of the joint.

Keywords: clinching, equivalent FE modelling, simplified elements, joining

1. Introduction

From both economical and environmental point of view, lightweight constructions have gained more interest in recent years. The need to join dissimilar, coated or hard to weld lightweight materials have led to rapid development of mechanical joining techniques such as clinched joints [1, 2, 3], self piercing rivets (SPR), riveting, etc. Clinching is a mechanical joining technique that involves severe local plastic deformation of two or more sheet metal parts using a punch and die. The local deformation results in a permanent mechanical interlock.

Email addresses: `andreas.breda@kuleuven.be` (Andreas Breda), `sam.coppieters@kuleuven.be` (Sam Coppieters), `dimitri.debruyne@kuleuven.be` (Dimitri Debruyne)

Clinching has been used on an industrial scale for over more than 35 years
10 and has been successfully applied to a wide variety of materials and material
combinations. Although several materials can be joined by clinching such as
steel[2, 4], aluminium alloys[5, 6], copper[7], magnesium[8], titanium[9], etc., an
important advantage of the joining technique is the possibility of joining dis-
15 similar materials. Several dissimilar materials have been successfully joined by
clinching including combinations with high strength steels[10, 11, 12], thermo-
plastic polymers[13], composite materials[12, 11] and wood[14]. Also, hybrid
joints, in which the clinch technology is combined with adhesives, has gained
interest in recent years[15, 16]. Although the patent was granted in 1897, re-
20 search and industrial interest started about 80 years later. The reason for this
is the complexity of the process, the wide variety of materials, combinations
and tools required to achieve the mechanical interlock. Additionally, the axial
strength of a clinched joint is limited compared to alternative joining techniques
[17]. The forming process, the influence of the tool geometry and the mechan-
ical performance of a single clinched joint have been extensively investigated
25 by finite element simulations [18, 4, 19, 20, 21, 22]. The clinched region is a
complex shaped zone where the material state varies from point to point. If
a structure or assembly contains many joints, it is unrealistic because of the
computational costs and means to build a numerical model containing a huge
number of detailed sub-models. The goal of this paper is to propose a method-
30 ology to replace the complex full-scale clinch model in numerical simulations
for quasi-static elastic-plastic loading (Fig. 1). The development of such an
equivalent model might enhance the analysis of specific applications such as:
clinched structures subjected to fatigue loads, design rules for clinched config-
urations and structural damage behaviour of clinched joints. Before focussing
35 on such applications, however, the focus in this paper is on the reproduction of
the global force displacement response up to maximum force to obtain a general
equivalent modelling procedure for a single clinched joint. Later, the procedure
can be extended, depending on the application at hand.

Simplified models were already successfully applied to other joining tech-
40 niques. To calibrate and/or validate these models, an experimental test, which
exposes the mechanical behaviour of the joint, is needed. For different join-
ing techniques, a modified Arcan test set-up is therefore often applied [23, 24,
25]. The modified Arcan test set-up consists of two disk halves, which can be
mounted in a uni-axial tensile machine under different angles, and was devel-
oped by Porcaro et al. [26] for riveted joints. Here, the modified Arcan fixture
45 can apply a mixed-mode loading onto the joint. For use with clinched joints, a
redesigned version of the modified Arcan set-up was developed by Coppieters
et al. [21].

A first simplified model for riveted joints, using the modified Arcan test
50 procedure, was proposed by Langrand et al. [23, 27]. A non-linear spring for-
mulation was used as an equivalent element and the parameters were calibrated
using the experimental results of the modified Arcan test. For self-piercing riv-
ets (SPR), Hanssen et al. [24] developed a point-connector model in an explicit
FEM code to be used in large scale crash simulations. The paper describes the

55 analytical definition of the model which entails 10 calibration parameters. These are determined from a peel test and the 0° , 45° and 90° modified Arcan test cases. Weyer et al. [25] suggested to use an equivalent SPR model for a crash analysis which reproduces the mechanical and damage behaviour of the joint. A simple fastener, provided in the ABAQUS code, is used and is calibrated
60 using experimentally acquired data from the modified Arcan test and peel test. Grujicic et al. [28, 29] extended this methodology and calibrated the equivalent model using a full scale numerical model of SPR test cases. For modelling assembly points in structures, Bérot et al. [30] proposed two universal equivalent elements, a connector based element and a virtual formulation. The calibration
65 procedure is based on 6 test cases from which the calibration parameters are derived using an optimisation algorithm.

For spot welds, different methodologies are successfully applied depending on the application. Xu et al. [31] evaluated the performance of different simplified spot weld models against detailed three-dimensional models, under linear
70 elastic load conditions. Five different load cases were evaluated (tension, out-of-plane torsion, out-of-plane bending, in-plane torsion and in-plane shear). Palmonella et al. [32] gives a brief overview of the simplified models used for spot welds in structural dynamics. The accuracy of six simplified spot weld models is updated using a finite element optimisation algorithm and two benchmark
75 structures (double hat and single hat structure) for validation and updating. Khandoker et al. [33] applied six different simplified spot weld models, using an experimental U-shaped pull-out test as validation method. The possibilities in this field for clinched joints, however, have not yet been thoroughly investigated. In a first step, a shear lap and several pull-out tests are evaluated to be
80 used as a reference case to characterize the mechanical behaviour of the joint. In a second step, an existing approach for SPR joints is adopted and evaluated for the use with clinched joints. As a final step, a modified methodology for a single clinched joint is proposed as proof of concept. This methodology is experimentally validated using a modified Arcan test and a peel test on both
85 DC01 steel and EN-AW 5754 aluminium alloy.

2. Experimental tests and set-up

2.1. Material properties

DC01 steel sheet is used in this work because it has excellent deep drawing properties [34], is widely available as sheet metal and therefore ideal for
90 clinch joining. In order to minimize the experimental work required for the proposed calibration method, the anisotropic properties of the base material are ignored and isotropic material behaviour of the DC01 steel sheet is assumed. As such, the elastic properties and strain hardening behaviour of DC01 sheet metal (thickness 1 mm) were obtained by means of a uni-axial tensile tests along the
95 rolling direction of the specimen only. Six samples (Fig. 2 b.) were cut out of the sheet plate to ensure the reproducibility of the test. The tensile test was performed using a tensile machine with a maximum capacity of 10 kN and a

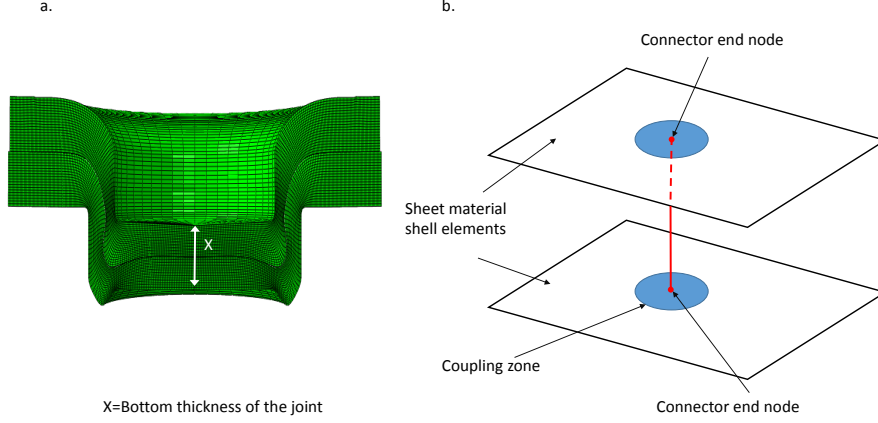


Figure 1: Principle of equivalent modeling: a. full scale model b. equivalent model

Manufacturer	Die number	Punch number	R_{DA}	R_P
Eckold	950.10	920.501	3 mm	2.5 mm

Table 1: Clinch tool specifications with die anvil radius (R_{DA}) and punch radius (R_P)

speed of 1 mm/min. The elongation was measured using an extensometer with a gauge length of 80 mm. The stress-strain results can be found in Fig. 2 a..
 100 An average Young's-modulus of 175544 N/mm² and hardening law were determined and used for the numerical simulation. The material was assumed to be elastically and plastically isotropic. The Swift law is of the following form:

$$\sigma_{eq} = 543.2(0.005549 + \epsilon_{eq}^{pl})^{0.2249} \quad (1)$$

Were σ_{eq} is the equivalent stress and ϵ_{eq}^{pl} is the plastic equivalent strain.

The material was joined with the Non Cutting Single Stroke (NCSS) clinch
 105 technology using an extensible die. Here, the die consists of two moving parts which enables the metal to flow in the radial direction during the clinch step, creating the mechanical interlock (Fig. 3). The details of the used tools can be found in table 1. The average clinch diameter was 8 mm with a bottom thickness of X=0.55 mm at the base of the joint. A section of the clinched joint
 110 can be seen in Fig. 4. In order to calibrate the numerical models, a reference test is necessary. Therefore a simple pull-out and shear lap experiment are performed on a clinched specimen. These experiments will be used to calibrate the equivalent numerical model of the clinched joint.

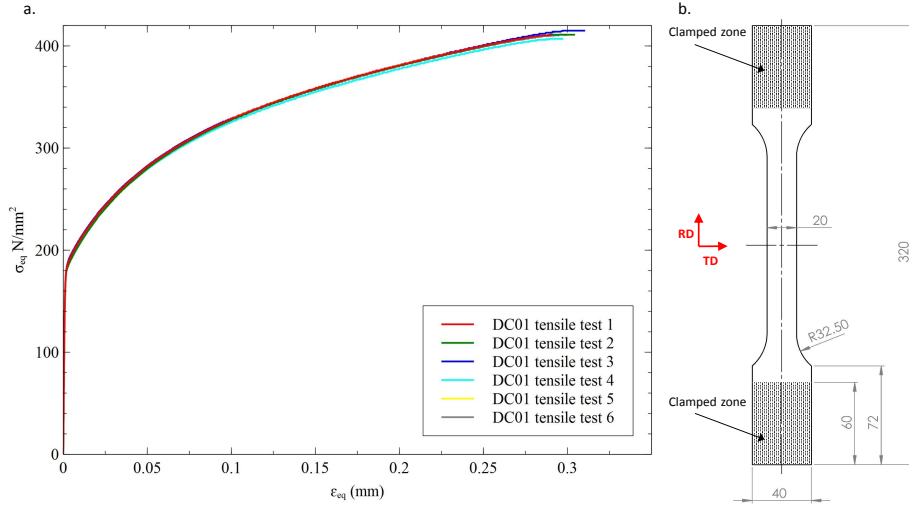


Figure 2: a. Stress strain curves DC01 in the rolling direction b. Dog bone specimen geometry (all dimensions in mm)

2.2. Pull-out test

115 During a pull-out test only axial loading is exerted onto the clinched joint. Three different type of pull-out tests have been investigated in order to identify the best reference test for calibrating the pull-out behaviour: Box test, cross tension test and H tension test [4, 1, 3]. A good pull-out calibration test for the equivalent model, exhibits a good ratio between sheet deformation in the zone
 120 surrounding the joint and intrinsic joint deformation. When a pull-out loading is exerted on a clinched joint, three failure modes can occur: neck fracture, failure by deformation of the interlock or a combination of both [35]. These joint intrinsic failure modes depend on the materials used, the tool geometry and the bottom thickness of the joint. The different failure modes, however,
 125 do not affect the sheet deformation behaviour substantially in a pull-out test. All pull-out tests were repeated 5 times to guarantee reproducibility. The test speed was set at 1 mm/min to obtain a quasi-static load case. The experimental results of the pull-out tests can be found in Fig. 7. All tests were conducted using a tensile machine with a capacity of 10 kN.

2.2.1. Box test

130 The box test set-up on a clinched joint was proposed by Coppieters et al. [19] to validate analytical calculations. The purpose of this test is to obtain the intrinsic joint behaviour under a pull-out load by constraining the specimen in the close vicinity of the joint. In this way, the inscribed radius of the material
 135 surrounding the joint is limited to a value of $R=8$ mm. The specimen is obtained by cutting a cruciform shape out of the DC01 sheet metal (Fig. 5 a.). The cruciform arms are then folded to a box shape and clinched together in the

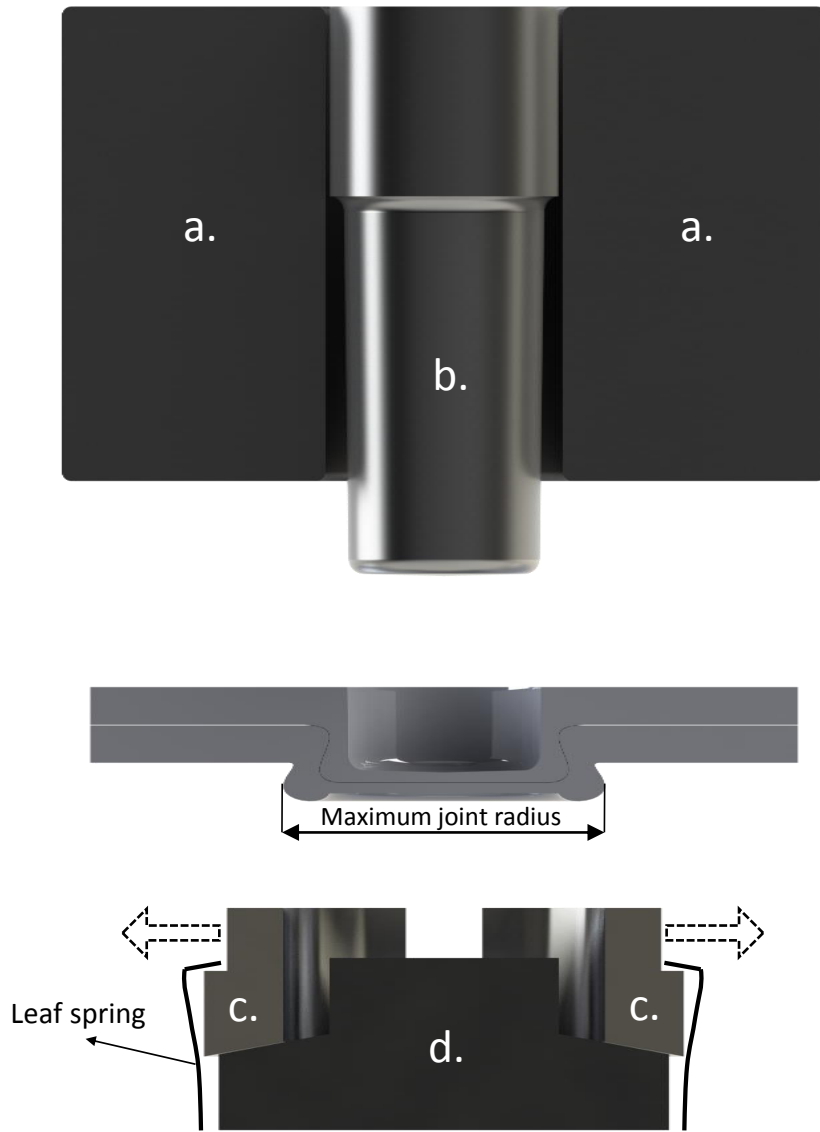


Figure 3: Tool geometrie: a. Stripper b. Punch c. Die segments d. Die anvil

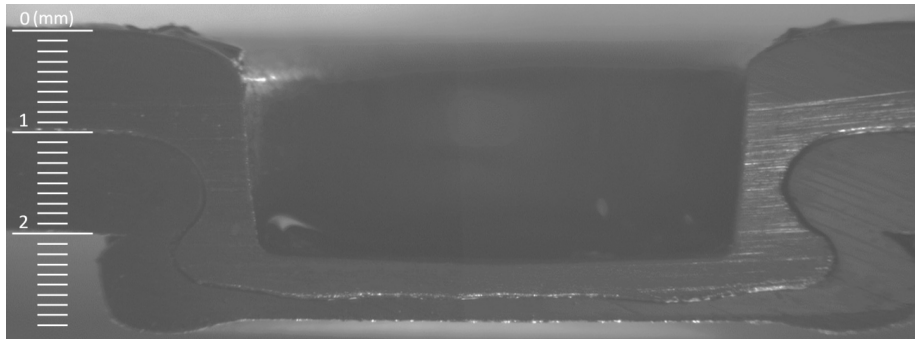


Figure 4: Section of the clinched joint in DC01 1 mm-1 mm sheet thickness

center of the specimen. The box specimen is bolted to a gauge clamp using washers to avoid slip during the test. This gauge clamp is mounted in a normal tensile machine. The elongation is measured using an extensometer with a gauge length of 70 mm. The results of the box test can be found in Fig. 7. It can be concluded that the deformation of the specimen is limited compared to other pull-out tests. Because of the constraint close to the joint, the material deformation surrounding the joint is very limited leading to a smaller elongation of the specimen. In practical clinch applications, however, it is very rare that sheet bending is completely restricted, due to the constraint that close to the joint. The force displacement response of the box test FE model is also very sensitive to the value of the inscribed radius and with that, it is also practically inconvenient to measure this radius correctly. Therefore, and because of the total deformation limited to the intrinsic joint properties, the box test is not appropriate as reference case for calibrating the equivalent model for clinched joints.

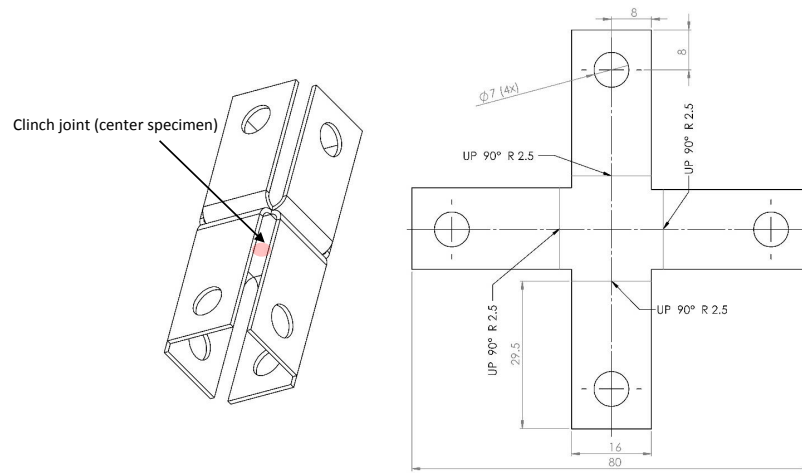
2.2.2. Cross tension test

The cross tension test proposes the most practical specimen for a pull-out test as a priori bending of the sheets is not necessary. Here, two rectangular sheets are clinched together so that a cruciform shape is obtained (Fig. 5 b.). The specimen is mounted within a uni-axial tensile machine using an auxiliary tool. The elongation is measured at a distance of 35 mm of the joint using an extensometer. The main disadvantage with this test is that severe local doming causes early failure of the joint and leads to unbuttoning of the joint [4]. This unbuttoning also has an influence on the intrinsic joint deformation which can hamper a representative calibration for the pull-out behaviour.

2.2.3. H tension test

In this type of pull-out test, two U shaped sheet specimen are clinched together so that a H tension specimen is obtained (Fig. 6 a.). This specimen is bolted to a clamping gauge using washers preventing slip of the specimen. The clamping gauge is mounted in a tensile machine and the elongation is measured

a.



b.

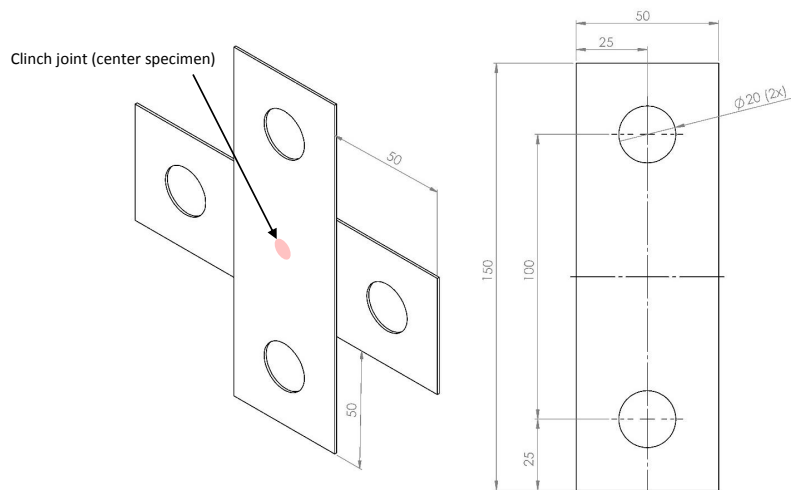
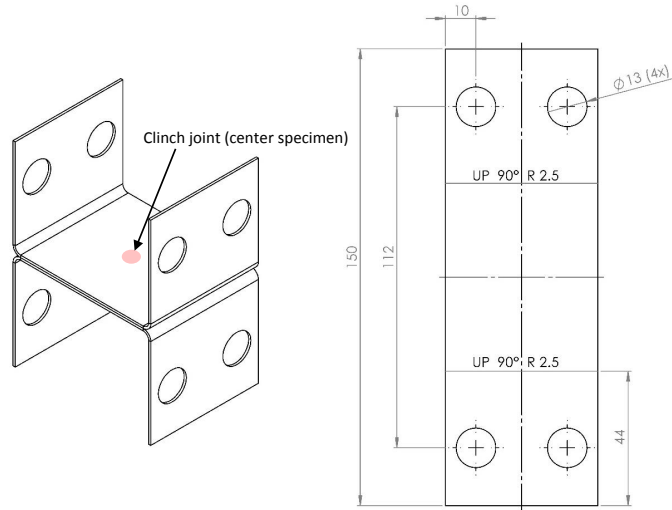


Figure 5: Overview of the considered pull-out tests set-up and geometry (all dimensions in mm): a. Box test b. Cross tension test

c.



d.

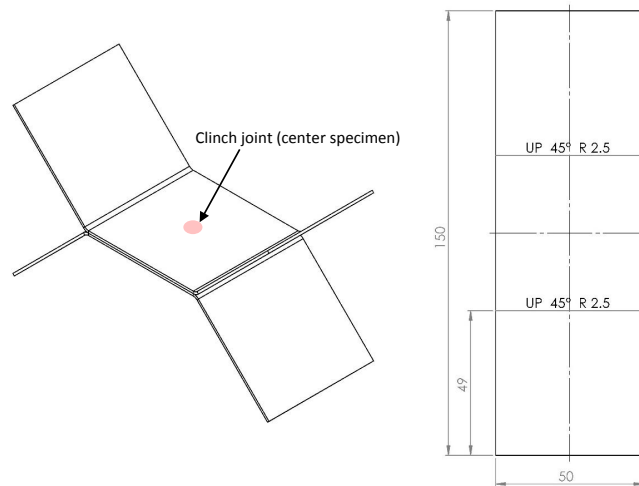


Figure 6: Overview of the considered pull-out tests set-up and geometry (all dimensions in mm): c. H tension test d. Modified Arcan 0° tension case

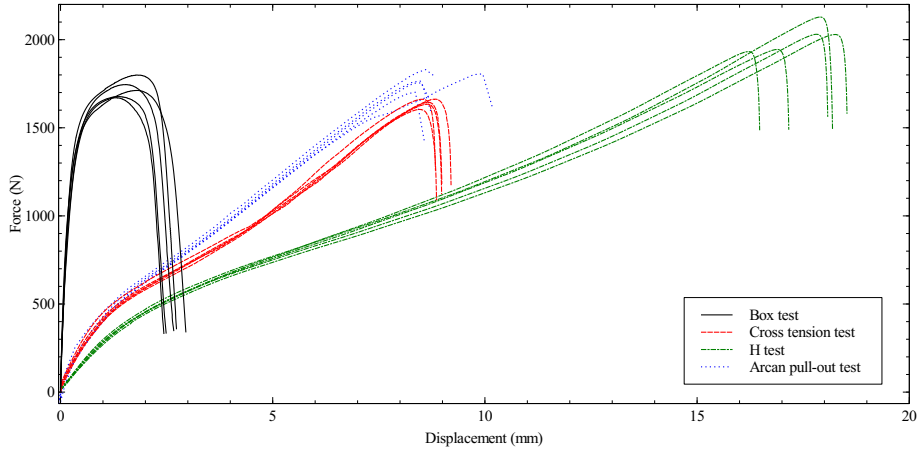


Figure 7: Pull-out tests overview

at a distance of 35 mm of the joint using an extensometer. During the H tension
 test, larger deformations of the sheet metal occur because the geometry of the
 specimen allows more sheet deformation compared to the other pull-out tests.
 170 The H tension test also yields a higher maximum load because the local doming
 effect is less significant compared to the cross tension test. This enables to
 identify the equivalent joint properties up to a higher load and can permit a
 better calibration of the joint behaviour. Consequently, the H tension test is a
 175 valid reference case for the pull-out behaviour. Because of the practical ease of
 use, this test will be used in this paper as the reference pull-out case.

2.2.4. Modified Arcan test pull-out case

The 0° modified Arcan test was shown to be equivalent as a pull-out test
 case [4]. The specimen geometry is similar to the one of the H tension test
 180 although instead of a U shape, the two sides of the sheet are bended in a
 45° angle to ensure mounting in the modified Arcan device (Fig. 6 b.). This
 device was mounted in a normal tensile machine with a maximum capacity of
 10 kN. Digital Image Correlation (DIC) was used to track the elongation of the
 modified Arcan fixture. This measurement was necessary because the use of
 185 an extensometer was practical inconvenient with this clamping gauge and the
 accuracy of the cross head was inaccurate when using mixed-mode loads. DIC
 is a contactless optical-numerical measurement technique which can determine
 displacement fields on a region of interest by taking camera images (Fig. 8 b.)
 of a random speckle pattern attached onto the specimen. By comparing the
 190 image from the undeformed state with the image from the deformed state, the
 displacement field can be calculated by the use of a correlation algorithm [36].
 The speckled zone was attached to the upper and lower clamp. The average
 displacement in these zones was taken (Fig. 8 c.) and synchronized with the
 force to determine the force-displacement behaviour of the specimen. The force

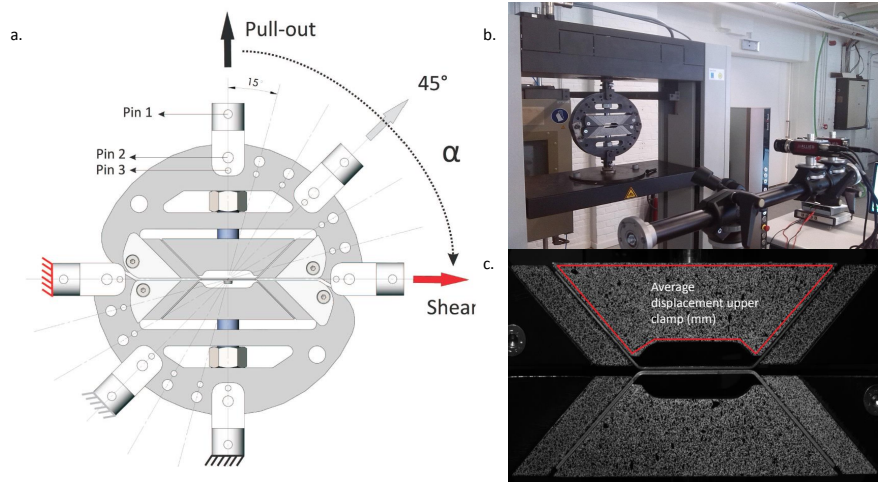


Figure 8: Modified Arcan set-up: a. Modified Arcan fixture b. Arcan test experimental set-up c. Speckle pattern for DIC

195 displacement results of the Arcan pull-out case are similar to the results of the
cross tension test (Fig. 7). It can be concluded that the maximum force is
higher compared to the cross tension test because the local doming effect is,
similar to the H-tension specimen, less pronounced in this test which makes this
test also valid to produce a representative pull-out test for the calibration of the
200 pull-out behaviour. However, with the DIC set-up and the more complex Arcan
fixture, the modified Arcan set-up is practically less convenient compared to the
H tension test.

2.3. Shear lap test

In order to understand and calibrate the joint behaviour under a shear load,
205 a shear lap test on a single joint was performed. The investigated joints solely
exhibited fracture in the neck. Therefore, and with only shear loads acting onto
the joint, the elongation of the sheet metal is limited compared to the pull-out
tests. Indeed, the deformation behaviour of a shear lap specimen is limited to
the intrinsic deformation of the joint. Unlike the pull-out test, the shear lap
210 test is less sensitive to the geometrical dimensions of the test specimen (Fig. 9
b.). The extensometer arms were each at a distance of 35 mm of the center of
the joint so that the initial gauge length equals 70 mm. The tensile test was
performed at 1 mm/min to obtain a quasi static load case. The results of the
test can be found in Fig. 9 a..

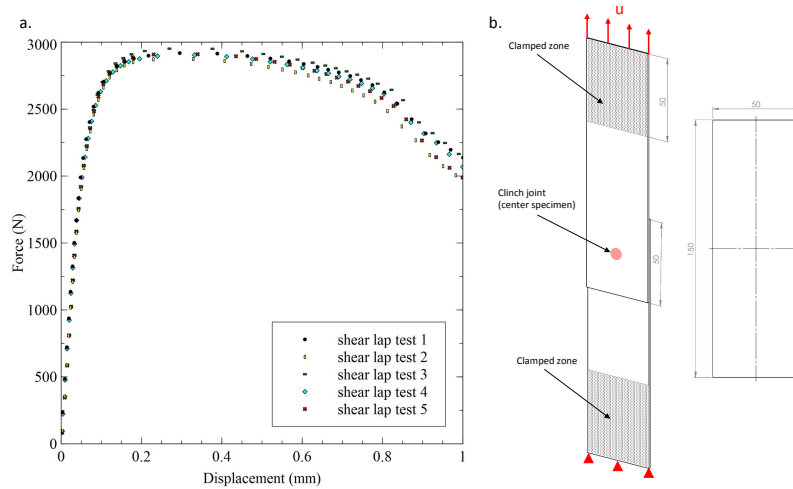


Figure 9: Shear lap test DC01 (all dimensions in mm): a. results b. specimen geometry

215 **3. Numerical model**

3.1. DC01 sheet material

The DC01 sheet material is modelled in the commercial FE code ABAQUS using linear shell elements with reduced integration and a thickness of 1 mm. A non-linear analysis was conducted using the ABAQUS/standard implicit solver.

220 The material properties from the tensile test are used to define the elastic and plastic material response of the DC01 sheets. Isotropic material behaviour is assumed. The validity of this assumption depends on the type of experiment and the specimen geometry. Planar anisotropy has an effect on the predicted force-elongation curve during a single shear lap test due to the local material state in the vicinity of the joint [19, 37].

225 The majority of the base material, however, is under elastic loading except for the plastic secondary bending which does not contribute to the strength of the joint and is limited for the joints considered in this paper due to the neck fracture failure mode . Local anisotropic effects are captured in the shear plastic calibration (section 5) of the equivalent model while

230 isotropic behaviour can be assumed for the majority of the base material. During the H tension test and the modified Arcan test, significant plastic deformation of the base material occurs. The effect on the force-displacement behaviour will depend on the level of plastic anisotropy and on the geometry of the test specimen. The observations and simulation results in this paper show that

235 the effect is moderate for the adopted test material and specimens. The local effects can again be captured during the calibration procedure and therefore the anisotropy of the base material can be safely ignored. An element size of 1 mm is required to reach convergence in the force-displacement results. The boundary conditions of the reference shear lap and pull-out test can be found

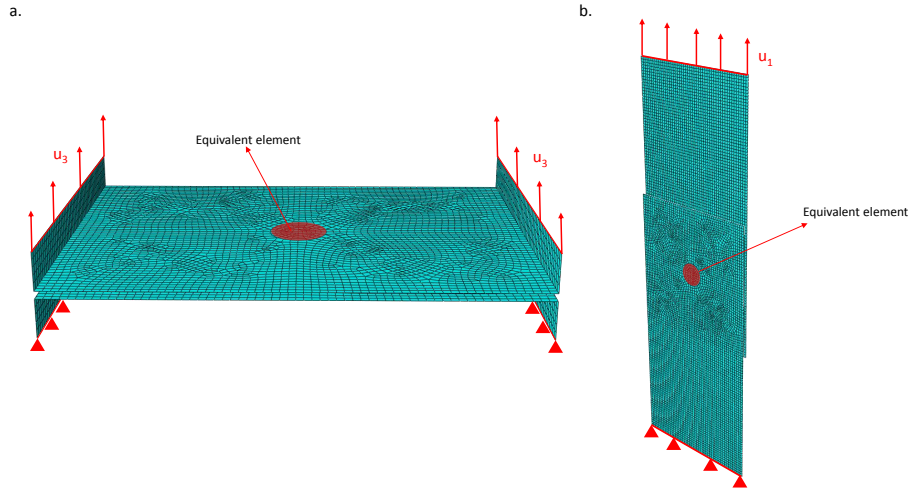


Figure 10: Numerical reference models: a. H tension test b. shear lap test

240 in Fig. 10.

3.2. Equivalent model representation

To model the clinched joint a connector formulation is used. This formulation has been proven to be optimal in terms of computational cost compared to a virtual element formulation [30]. The connector formulation consists of a beam like connection with a local coordinate system and 6 degrees of relative motion ($U1, U2, U3, UR1, UR2, UR3$), all in which elastic and plastic behaviour can be introduced. The end nodes of this connector are coupled to a coupling zone onto the shell elements which acts as the clinched joint influence area on the sheet material (Fig. 11). For SPR, Weyer et al. [25] suggested to couple the end nodes of the connector with the influence zone using a structural distributing coupling. This coupling distributes the moments and forces acting on the connector over the elements of the influence area which can cause local deformation of the coupling zone. As a result, the model will have a lower stiffness compared with the experimental results (Fig. 12). It can be concluded that the influence zone of the clinched joint can be represented as a rigid zone inside the sheet material. The use of a kinematic coupling is therefore a good approximation for a clinched joint (Fig. 12). Increasing the radius of the influence zone will lead to a stiffer behaviour of the pull-out FE model as it limits the deformation of the sheet metal surrounding the clinched joint. In order to respect the physical dimensions of the joint, the influence zone radius is assumed equal to the maximum clinch radius as can be seen in Fig. 3.

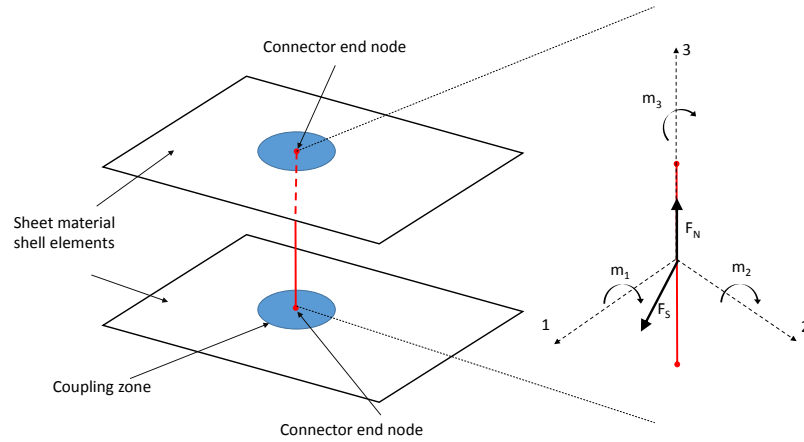


Figure 11: Connector schematic representation

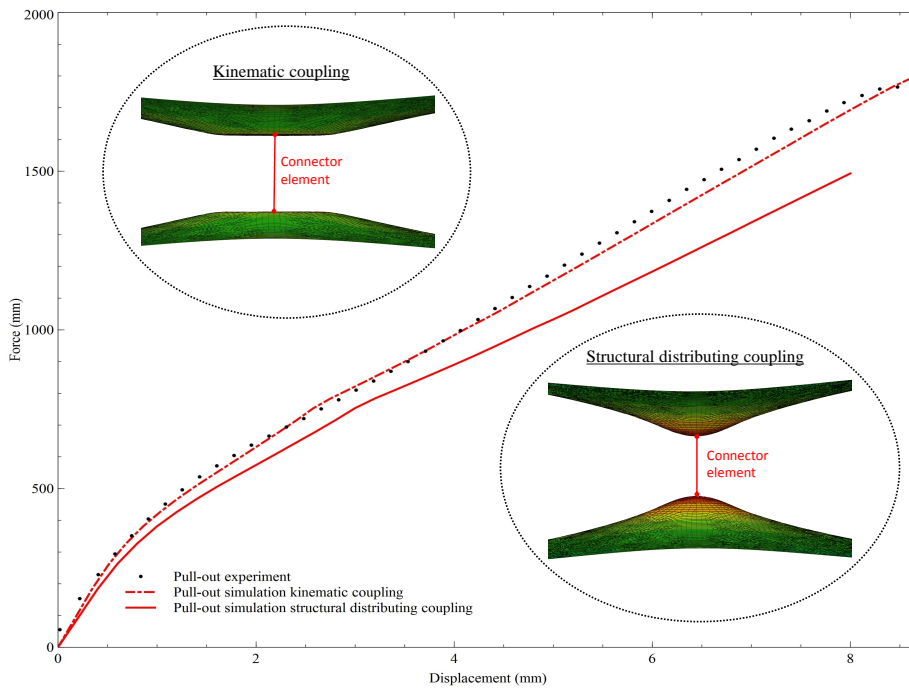


Figure 12: Coupling methods: a. Structural distributing coupling b. Kinematic coupling

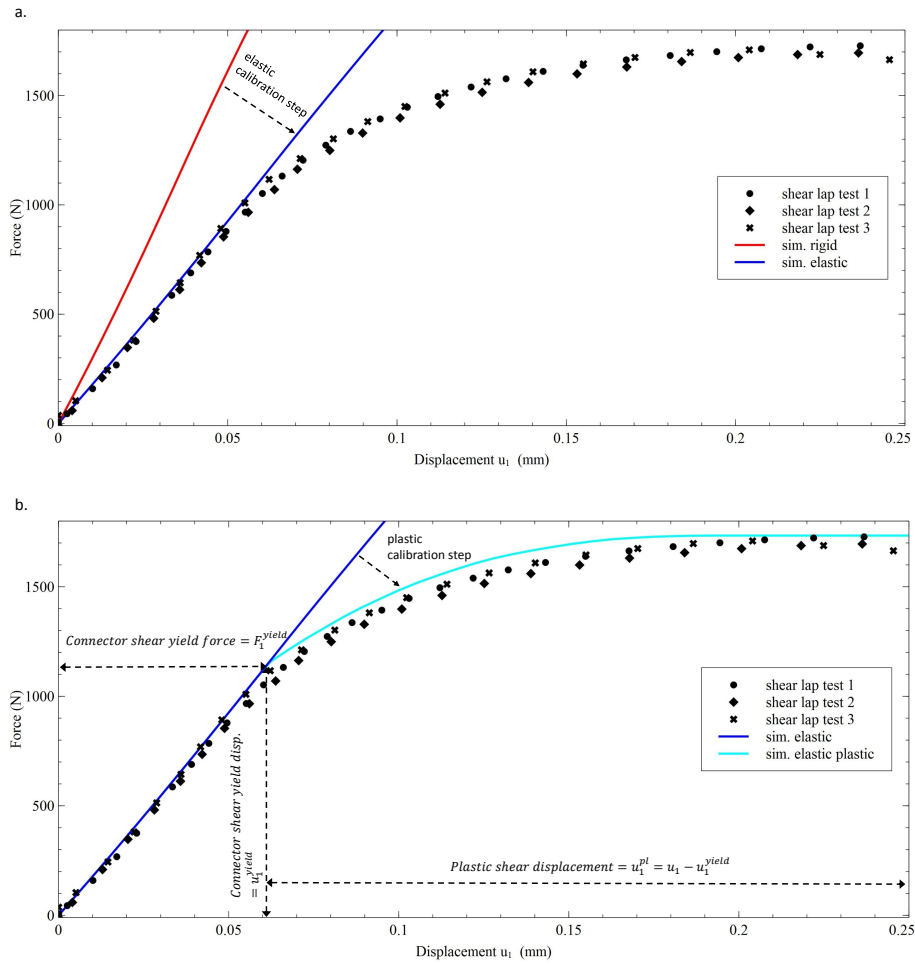


Figure 13: Connector calibration step (shear behaviour) using the shear lap test experimental results (equal steps for the normal behaviour): a. Elastic calibration step b. Plastic calibration step

4. Connector elastic behaviour calibration

Uncoupled elastic behaviour is used meaning that the spring stiffness's D_{ii} are defined independently for each load direction. The following equation is used to calculate the elastic response of the connector:

$$F_i = D_{ii} \cdot u_i \quad (2)$$

With D_{U1} , D_{U2} and D_{U3} , the two shear and the normal stiffness's of the connector, respectively. To calibrate the latter stiffness's a rigid stiffness is initially assumed as connector section in both numerical models of the reference tests. Through comparison with the experimental force displacement curves of the shear lap and pull-out tests, the connector stiffness is calibrated (Fig. 13 a.). Due to the limited rotation of the clinched joint, D_{UR1} and D_{UR2} (rotation around the radial axes) are assumed to be rigid. The rotation around the normal axis, D_{UR3} , is assumed to be free as the joint can rotate around the normal axis with limited amount of resistance.

5. Connector plastic behaviour calibration

5.1. Coupled plastic behaviour

5.1.1. Definition and implementation

Weyer et al. [25] presented a methodology for SPR joints based on coupled plastic behaviour for the connector plasticity. This methodology could potentially be interesting for clinched joints, as the plastic behaviour requires only one reference test case (shear lap experiment) to calibrate the plastic behaviour. Using this methodology, all the forces and moments exerted to the connector are coupled in a connector potential function $P(f)$ which determines the yield surface of the connector. The yield function is of following form:

$$\phi(\mathbf{f}, \bar{u}^{pl}) = P(\mathbf{f}) - F^0(\bar{u}^{pl}) \quad (3)$$

The potential function uses the equivalent normal force F_N and equivalent shear force F_S to calculate the connector potential and is of following general form:

$$P = ((F_N/R_N)^\beta + (F_S/R_S)^\beta)^{1/\beta} \quad (4)$$

with

$$F_N = |f_3| + K\sqrt{m_1^2 + m_2^2} \quad (5)$$

$$F_S = \sqrt{f_2^2 + f_3^2} \quad (6)$$

Where f_1, f_2, f_3, m_1 and m_2 are the connector forces and moments as shown in Fig. 11. K is a parameter to determine the contribution of the bending moments m_1 and m_2 to the connector potential. This term can be ignored, as the bending moments are negligible in the considered pull-out and shear lap

test. To normalise the equivalent shear and equivalent normal forces, a normal scaling factor $R_N=20$ and a shear scaling factor $R_S=29$ are derived from the average maximum normal force (pull-out test) and average maximum shear force (shear lap test), respectively. The exponent β determines the shape of the yield function. Weyer et al. calibrated this parameter using the modified Arcan test results for mixed-mode loads. For pure normal and pure shear forces acting onto the connector, the change in β value has no influence on the yielding of the connector as can be seen in Fig. 14. As the calibration step is done using the shear lap test results and the validation step considered in this section uses the pull-out test results, β has no influence on the calibration procedure or on the validation simulation results. The default β value of 2 was arbitrarily chosen to be used in the connector potential equation. This leads to a connector potential of following form:

$$P = ((F_N/20)^2 + (F_S/29)^2)^{1/2} \quad (7)$$

For the connector hardening, an equivalent hardening law is defined. Isotropic hardening is assumed for the connector and is defined as a tabular function of the equivalent force F^0 as a function of the equivalent plastic motion \bar{u}^{pl} :

$$\bar{u}^{pl} = \int_0^t \dot{\bar{u}}^{pl} dt \quad (8)$$

As soon as yielding occurs, the associated plastic flow rule:

$$\dot{\mathbf{u}}^{pl} = \dot{\bar{u}}^{pl} \cdot \frac{\partial \phi}{\partial \mathbf{f}} \quad (9)$$

was used to derive and calculate the plastic relative motion of the connector u_i^{pl} . With $\dot{\mathbf{u}}^{pl}$ the plastic motion rate of all the connector components used in equations (5) and (6).

$\dot{\bar{u}}^{pl}$ is the equivalent plastic relative motion rate and can be derived from equation (9):

$$\dot{\bar{u}}^{pl} = \sqrt{\dot{\mathbf{u}}^{plT} \cdot \dot{\mathbf{u}}^{pl} / \left(\frac{\partial \phi}{\partial \mathbf{f}^T} \cdot \frac{\partial \phi}{\partial \mathbf{f}} \right)} \quad (10)$$

Weyer et al. [25] proposed to use the shear lap test as a reference case for SPR to calibrate the equivalent hardening law $F^0(\bar{u}^{pl})$. If equations (9) and (10) are applied for pure shear forces acting onto the connector in the shear lap experiment, the following equation for \bar{u}^{pl} can be derived:

$$\bar{u}^{pl} = R_S \cdot u_1^{pl} \quad (11)$$

For pure shear forces, following equations for the equivalent yield force can be derived from equations (3) and (4):

$$F^0 = \frac{F_S}{R_S} \quad (12)$$

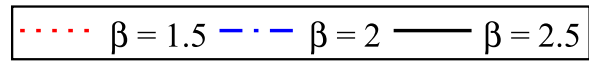
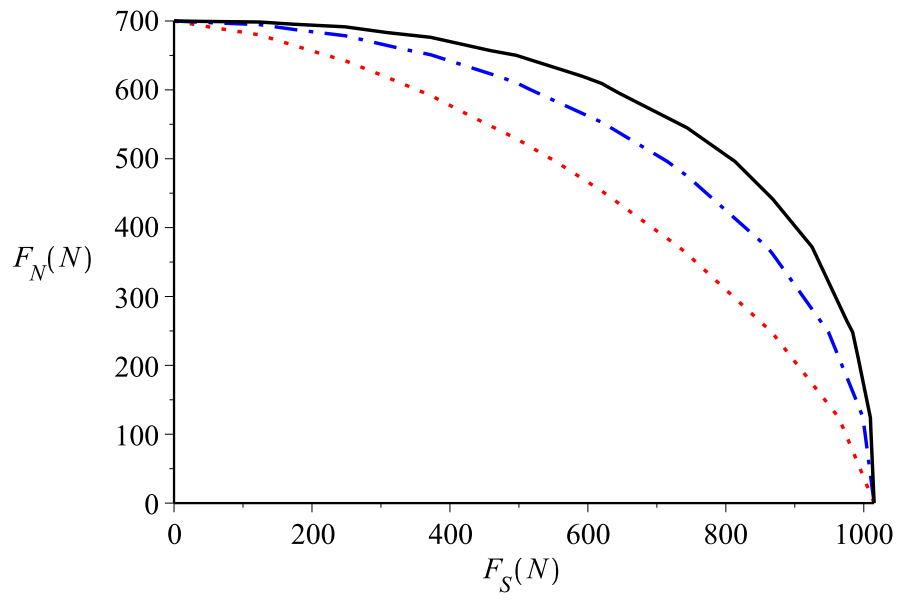


Figure 14: Yield surface connector for different beta values

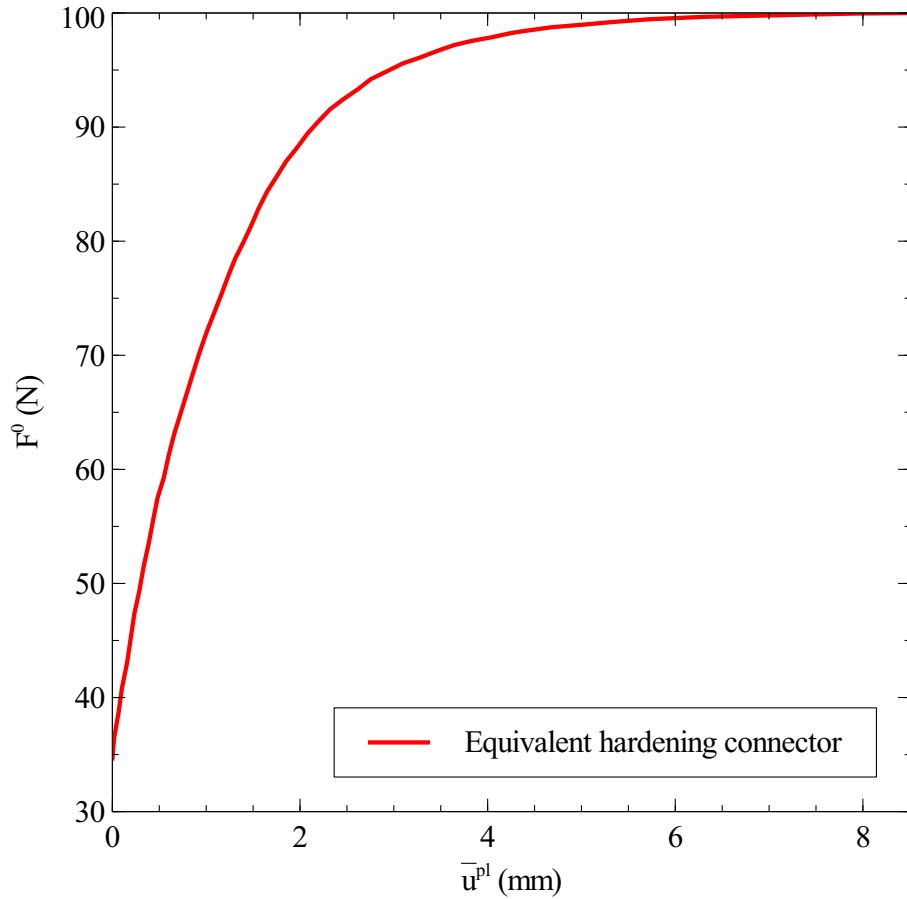


Figure 15: Calibrated connector equivalent hardening law, using the shear lap experimental results

If equations (11) and (12) are applied for the reference shear lap test, a tabular equivalent hardening law is obtained for the connector (Fig. 15).

5.1.2. Validation

If the calibrated coupled plasticity based on the shear test is applied to the pull-out test as validation, it can be concluded that the equivalent hardening law acts too stiff in a pull-out test on a clinched joint (Fig. 16). The reason for that is, with coupled plastic behaviour, the transformation to another load direction of the equivalent plastic displacements uses the yield potential. For the pull-out case, only an equivalent scaling factor R_N is used to scale the plastic displacements, which is insufficient to obtain a universal hardening law for an equivalent clinch model.

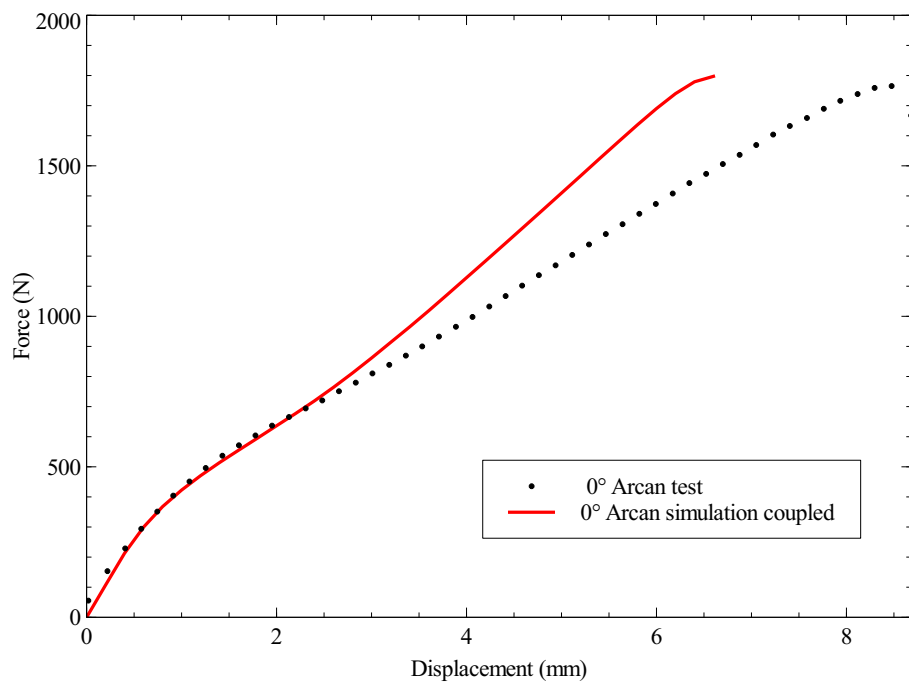


Figure 16: Arcan 0° coupled behaviour simulation results

Radius	D_{U1}	D_{U2}	D_{U3}	D_{UR1}	D_{UR2}	D_{UR3}	$K_{u,N}$	$K_{u,S}$
4 mm	rigid	rigid	rigid	rigid	rigid	free	0.4	0.7

Table 2: Calibration parameters DC01 equivalent model

5.2. Uncoupled plastic behaviour

5.2.1. Definition and implementation

As coupled connector plasticity was proven in the previous section to be
335 insufficient for a clinched joint, another implementation method is proposed.
To describe the plastic behaviour of the connector element, an independent
force-displacement based hardening law is proposed for each of the main load
directions (shear and normal) exerted to the connector. By using this defini-
tion, the force displacement hardening law is allowed to differ substantially in
340 shape compared to the coupled definition, dependent of the loading direction.
For mixed-mode load conditions, the plastic connector deformation acts as the
resultant of both hardening laws. These hardening laws are calibrated using
the experimental results of the reference pull-out and shear lap tests (Fig. 13
b.). The yielding force of the connector can directly be derived from matching
345 the shear lap and pull-out elastic connector simulations with the experimental
reference results (equation 13 and 15). The plastic displacements u_1^{pl} and u_3^{pl} ,
however, retrieved from the experimental reference cases, need scaling factors
 $K_{u,N}$ and $K_{u,S}$ (equation 14 and 16) to determine the correct displacements u_S^{pl}
and u_N^{pl} at the connector end nodes. Indeed, it is physically impossible to obtain
350 the latter values directly from the reference experiments, and, consequently, a
scaling factor K needs to be introduced. The specimen geometry and type of
test determine the size of the scaling factor. By matching the simulations with
the reference case experiments, the scaling factors and hardening laws are deter-
mined. The resulting connector hardening laws are independent of the specimen
355 geometry and size. The calibrated parameters for the DC01 joint can be seen
in Table 2.

For the normal direction:

$$F_N = f_3 \quad (13)$$

$$u_N^{pl} = u_3^{pl} \cdot K_{u,N} \quad (14)$$

For the shear direction:

$$F_S = f_1 = f_2 \quad (15)$$

$$360 \quad u_S^{pl} = u_1^{pl} \cdot K_{u,S} \quad (16)$$

5.2.2. Validation

To validate the equivalent model for clinched connections presented in section
5.2.1, a modified Arcan test under different angles and a peel test are both
simulated and conducted. All tests were conducted using a uni-axial tensile
365 machine with a force capacity of 10 kN.

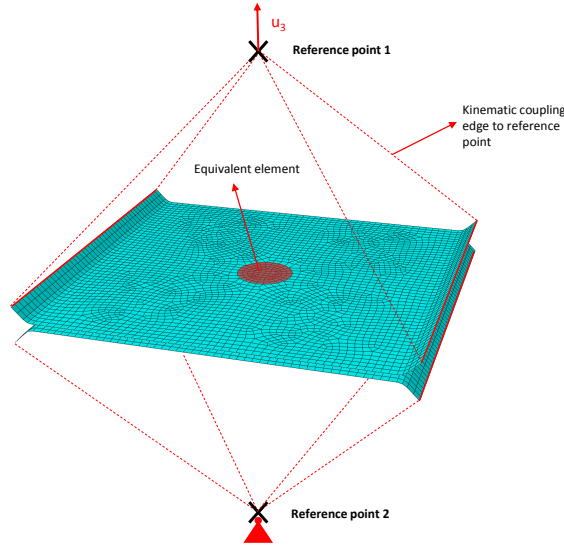


Figure 17: Arcan test finite element model (pull-out case)

Arcan test. In practice, the clinched joint will be exposed to a combination of shear and pull-out loads. In order to validate the calibrated joint behaviour, mixed-mode load conditions need to be applied to the joint. To achieve that, a modified Arcan test was performed for 3 different load cases (30°, 60°, 45°).
 370 This test has been widely accepted as validation method for equivalent models [23, 24, 25]. Our in-house produced modified Arcan fixture was mounted in a single axis tensile machine. Pin 3 (Fig. 8 a.) was omitted in order to permit rotation of the fixture during the test. The test speed was set at 1 mm/min to obtain a quasi-static load. The finite element model of the test can be found
 375 in Fig. 17. In accordance to the experimental set-up, the rotation in the plane of the fixture was permitted in the reference points of the finite element model. The simulation results of the Arcan test (Fig. 18 a.) show that the presented methodology for clinched joints gives an accurate prediction of the global force-displacement behaviour of the clinched specimen up to maximum force. The
 380 implementation of the uncoupled elastic-plastic behaviour is therefore able to reproduce the joints behaviour in case of mixed-mode loads.

Peel test. Additionally, the influence of bending moments was investigated using a peel test on a clinched specimen. The geometry of the specimen can be seen in Fig. 19 b.. The elongation was measured using an extensometer with a gauge
 385 length of 40 mm. Comparing the results of the simulation with the experiment

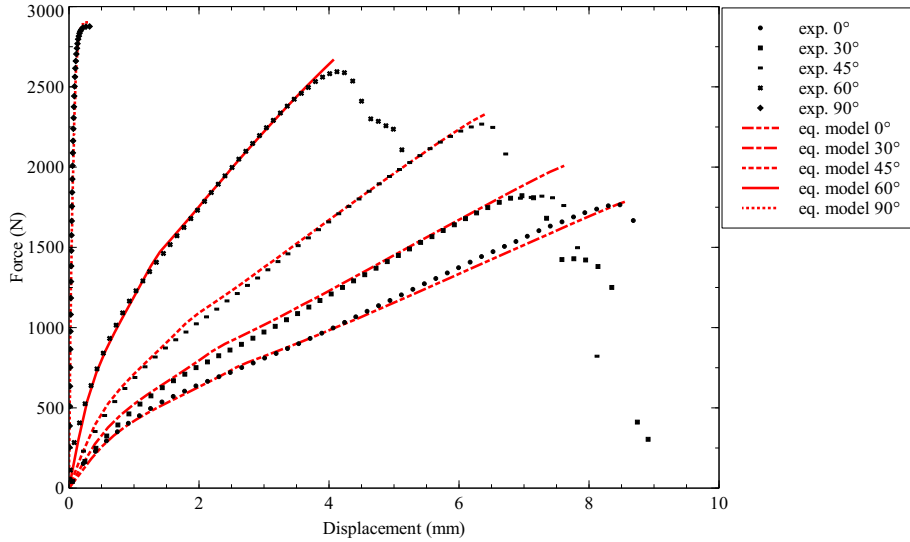


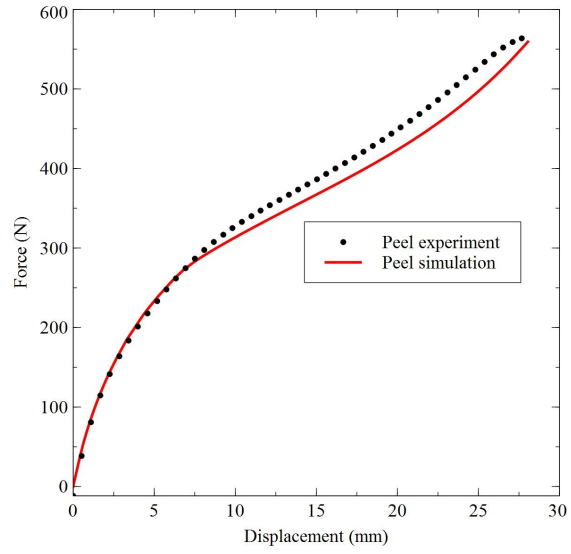
Figure 18: DC01 Arcan validation test+simulation results

(Fig. 19 a.), it can be concluded that the moments acting onto the joint have no substantial influence on the intrinsic deformation behaviour of the joint as the equivalent formulation does not include bending moments and is still able to reproduce the force displacement response. The moments acting onto the joint, however, will cause early failure of the joint compared to a pure pull-out mode.

6. Influence of materials and clinch tools

In order to validate the method using different base material and clinch tools, the methodology was applied to a clinched joint connection in an aluminium alloy. EN AW 5754 H111 sheet material of thickness 1.5 mm was used. The tool set used to join this aluminium differs from the DC01 material. The die used for this joint was a closed die with a radius of 4 mm resulting in different mechanical properties of the joint. A shear lap test and H-tension test was conducted in order to calibrate the equivalent model behaviour using the uncoupled elastic-plastic methodology proposed in section 5.2. The calibrated values for the equivalent model are shown in Table 3. A peel test and modified Arcan test were performed on the joint to validate the simulation results. During the modified Arcan test and peel test, the shear and pull-out failure mode was limited to neck rupture. No clear "failure by deformation of the interlock" only could be distinguished. The modified Arcan test results can be found in Fig. 20. Furthermore, from the modified Arcan test results, it can be concluded that the maximum strength of the joint did not increase substantially when the load case changed from pure pull-out to shear compared to the DC01 material. It can be concluded that for a different material/tool combination, the methodology can

a.



b.

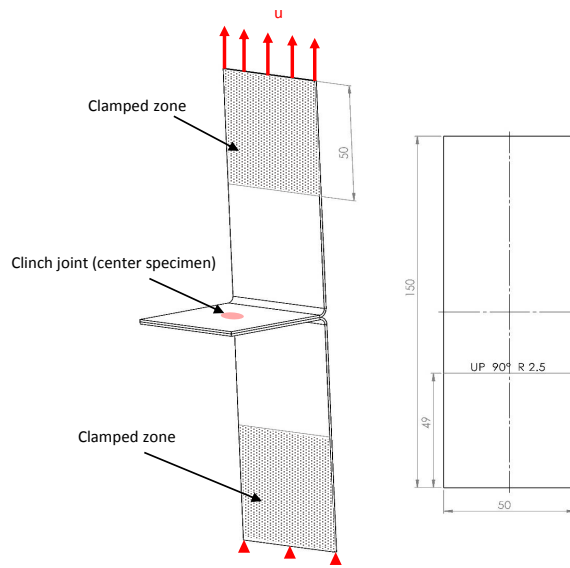


Figure 19: DC01 peel test (all dimensions in mm): a. Results b. Peel specimen geometry

Radius	D_{U1}	D_{U2}	D_{U3}	D_{UR1}	D_{UR2}	D_{UR3}	$K_{u,N}$	$K_{u,S}$
4.35 mm	4500 N/mm	4500 N/mm	2500 N/mm	rigid	rigid	free	0.4	0.5

Table 3: Calibration parameters EN AW 5754 equivalent model

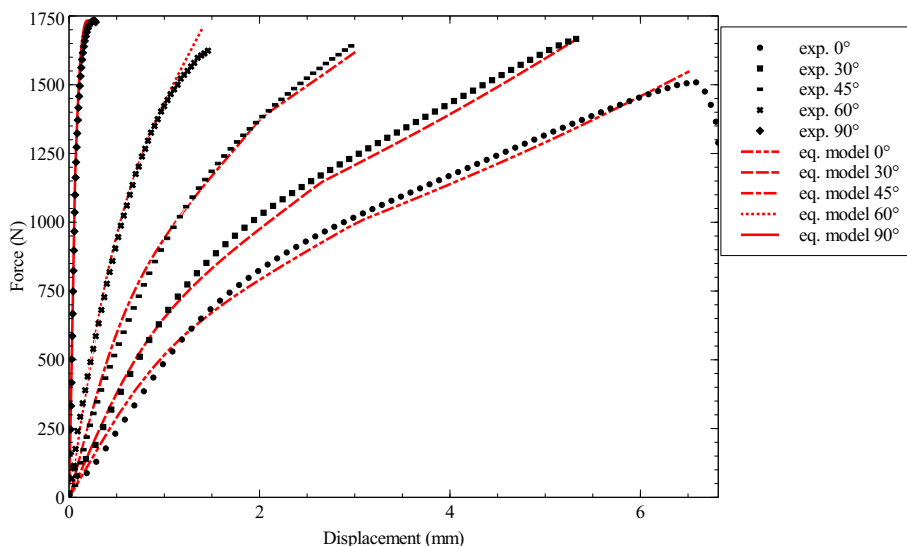


Figure 20: EN AW 5754 H111 Arcan validation test+simulation results

reproduce the force-displacement response for mixed-mode load cases. The peel
410 test results can be found in Fig. 21. Here, as with the DC01 material, it can be
concluded that the moments acting on the joint have no substantial influence
on the deformation behaviour and the equivalent model is able to reproduce the
response of the joint.

7. Conclusion

415 An equivalent modelling strategy is developed to describe the general static
mechanical behaviour of a clinched joint up to maximum force or damage ini-
tiation. The simplified model uses a connector formulation combined with a
kinematic coupling to establish the equivalent representation of a clinched joint.
Uncoupled plastic behaviour is proposed to simulate the elastic-plastic proper-
420 ties of the connector. The simulation of the modified Arcan test on a single
clinched joint, in DC01 and EN AW 5754 sheet material, validates the proposed
methodology and enables to reproduce the mechanical behaviour of the tested
specimen up to maximum force. It can therefore be concluded that the inde-
pendent or uncoupled elasticity and plastic hardening, calibrated using a simple
425 shear lap test and H tension test, is a good approximation to describe the be-

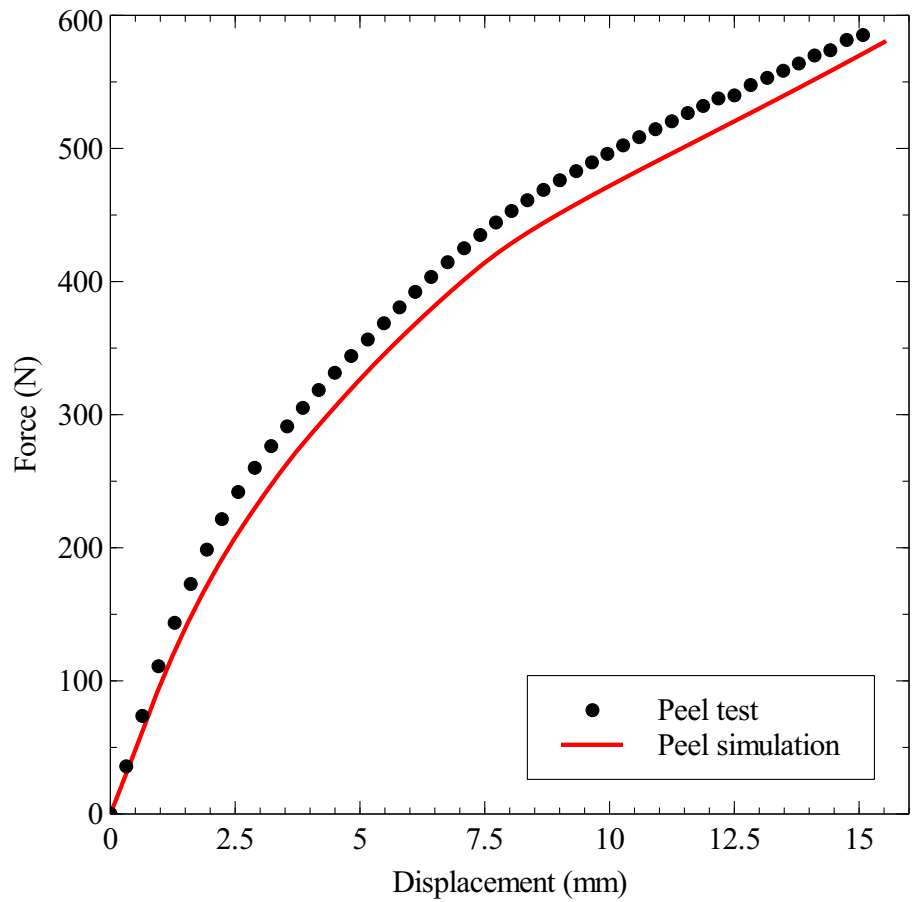


Figure 21: EN-AW 5754 Peel test results

haviour of a clinched joint. The use of coupled plastic behaviour, however, is proven to be insufficient for clinched joints. Isotropic material behaviour can be assumed to model the experiments presented in this paper. However, for excessive base material deformations, other geometries or joint failure modes, the anisotropic properties may need to be considered. This will be scrutinized in future work.

The proposed modelling strategy provides a first step to investigate the possibilities of an equivalent model in modelling large structures where clinched joints are present. Research to extend the presented methodology to structures containing a large number of clinched joints is under way. For this application, a modification of the equivalent model may be required as interaction effects can possibly cause a change in the deformation behaviour of the joint. Also for fatigue applications of clinched joints where maximum forces are lower than the ones presented, this methodology can provide a good basis for an equivalent fatigue model. Work along these lines is currently under way and will be published in forthcoming papers.

References

- [1] S. Coppieters, D. Debruyne, Clinching as interesting alternative for spot welding, Tech. rep., KU Leuven (2012).
- [2] J. P. Jaspart, T. Meyer, T. Mononen, R. Schneider, T. Toma, D. White, T. Leino, Novel jointing systems for the automated production of light gauge steel elements, Tech. rep., European Commission (2003).
- [3] S. Coppieters, D. Debruyne, Clinching.net, www.clinching.net, 2012.
- [4] S. Coppieters, Experimental and numerical study of clinched connections, Ph.D. thesis, KU Leuven (2012).
- [5] F. Lambiase, A. Di Ilio, A. Paoletti, Joining aluminium alloys with reduced ductility by mechanical clinching, *The International Journal of Advanced Manufacturing Technology* 77 (2015) 1295–1304.
- [6] F. Lambiase, A. Di Ilio, Damage analysis in mechanical clinching: Experimental and numerical study, *Journal of Materials Processing Technology* 230 (2016) 109 – 120.
- [7] X. Baoying, H. Xiaocong, W. Yuqi, Y. Huiyan, D. Chengjiang, Study of mechanical properties for copper alloy h62 sheets joined by self-piercing riveting and clinching, *Journal of Materials Processing Technology* 216 (2015) 28 – 36.
- [8] R. Neugebauer, C. Kraus, S. Dietrich, Advances in mechanical joining of magnesium, *CIRP Annals - Manufacturing Technology* 57 (2008) 283 – 286.
- [9] L. Zhao, X. C. He, Y. Lu, Study on clinching of titanium alloy, *Applied Mechanics and Materials* 633-634 (2014) 86–89.

- 465 [10] C.-J. Lee, J.-Y. Kim, S.-K. Lee, D.-C. Ko, B.-M. Kim, Parametric study on mechanical clinching process for joining aluminum alloy and high-strength steel sheets, *Journal of Mechanical Science and Technology* 24 (2010) 123–126.
- [11] C.-J. Lee, J.-M. Lee, H.-Y. Ryu, K.-H. Lee, B.-M. Kim, D.-C. Ko, Design
470 of hole-clinching process for joining of dissimilar materials al6061-t4 alloy with dp780 steel, hot-pressed 22mnb5 steel, and carbon fiber reinforced plastic, *Journal of Materials Processing Technology* 214 (2014) 2169 – 2178.
- [12] S.-H. Lee, C.-J. Lee, K.-H. Lee, J.-M. Lee, B.-M. Kim, D.-C. Ko, Influence of tool shape on hole clinching for carbon fiber-reinforced plastic and sprc440, *Advances in Mechanical Engineering* 6 (2014) 1–12.
475
- [13] F. Lambiase, A. Di Ilio, Mechanical clinching of metalpolymer joints, *Journal of Materials Processing Technology* 215 (2015) 12 – 19.
- [14] S. Lüder, S. Härtel, C. Binotsch, B. Awiszus, Influence of the moisture content on flat-clinch connection of wood materials and aluminium, *Journal of Materials Processing Technology* 214 (2014) 2069 – 2074.
480
- [15] F. Moroni, A. Pirondi, F. Kleiner, Experimental analysis and comparison of the strength of simple and hybrid structural joints, *International Journal of Adhesion and Adhesives* 30 (2010) 367 – 379.
- [16] T. Balawender, T. Sadowski, P. Golewski, Numerical analysis and experiments of the clinch-bonded joint subjected to uniaxial tension, *Computational Materials Science* 64 (2012) 270 – 272.
485
- [17] K. Mori, Y. Abe, T. Kato, Mechanism of superiority of fatigue strength for aluminium alloy sheets joined by mechanical clinching and self-pierce riveting, *Journal of Materials Processing Technology* 212 (9) (2012) 1900 – 1905.
490
- [18] X. He, Recent development in finite element analysis of clinched joints, *Int. J. Adv. Manuf. Tech.* 48 (2009) 607–612.
- [19] S. Coppieters, S. Cooreman, P. Lava, H. Sol, P. Van Houtte, D. Debruyne, Reproducing the experimental pull-out and shear strength of clinched sheet metal connections using fea, *International Journal of Material Forming* 4 (2011) 429–440.
495
- [20] S. Coppieters, P. Lava, S. Baes, H. Sol, P. Van Houtte, D. Debruyne, Analytical method to predict the pull-out strength of clinched connections, *Thin Walled Structures* 52 (2012) 42–52.
- 500 [21] S. Coppieters, P. Lava, R. Van Hecke, S. Cooreman, H. Sol, P. Van Houtte, D. Debruyne, Numerical and experimental study of the multi-axial quasi-static strength of clinched connections, *International Journal of Material Forming* 6 (2013) 437–451.

- 505 [22] F. Lambiase, Influence of process parameters in mechanical clinching with extensible dies, *The International Journal of Advanced Manufacturing Technology* 66 (2013) 2123–2131.
- [23] B. Langrand, L. Patronelli, E. Deletombe, E. Markiewicz, P. Draztic, An alternative numerical approach for full scale characterisation for riveted joint design, *Aerosp. Sci. Technol.* 6 (2002) 343–354.
- 510 [24] A. G. Hanssen, L. Olovsson, R. Porcaro, M. Langseth, A large-scale finite element point-connector model for self-piercing rivet connections, *European Journal of Mechanics - A/Solids* 29 (2010) 484–495.
- [25] S. Weyer, H. Hooputra, F. Zhou, Modeling of self-piercing rivets using fasteners in crash analysis, in: 2006 ABAQUS Users' Conference, 2006.
- 515 [26] R. Porcaro, A. G. Hanssen, M. Langseth, A. Aalberg, The behaviour of a self-piercing riveted connection under quasi-static loading conditions, *International Journal of Solids and Structures* 43 (2006) 5110–5131.
- [27] B. Langrand, E. Deletombe, E. Markiewicz, P. Draztic, Riveted joint modeling for numerical analysis of airframe crashworthiness, *Finite Elements in Analysis and Design* 38 (2001) 21–44.
- 520 [28] M. Grujicic, J. Snipes, S. Ramaswami, F. Abu-Farha, Self-piercing riveting process and joint modeling and simulations, *SAS* 3 (2014) 20–29.
- [29] M. Grujicic, J. Snipes, S. Ramaswami, Process modeling, joint-property characterization and construction of joint connector for mechanical fastening by self-piercing riveting, *Multidiscipline Model. Mater. Struct.* 10 (2014) 631–658.
- 525 [30] M. Bérot, J. Malrieu, F. Bay, An innovative strategy to create equivalent elements for modelling assembly points in joined structures, *Eng. Computation.* 31 (2014) 453–466.
- 530 [31] S. Xu, X. Deng, An evaluation of simplified finite element models for spot-welded joints, *Finite Elements in Analysis and Design* 40 (2004) 1175–1194.
- [32] M. Palmonella, M. I. Friswell, J. E. Mottershead, A. W. Lees, Finite element models of spot welds in structural dynamics: review and updating, *Computers and Structures* 83 (2005) 648–661.
- 535 [33] N. Khandoker, M. Takla, Tensile strength and failure simulation of simplified spot weld models, *Materials and Design* 54 (2014) 323–330.
- [34] H. Gürün, d. Karaağaç, The experimental investigation of effects of multiple parameters on the formability of the dc01 sheet metal, *Journal of Mechanical Engineering* 61 (2015) 651–662.

- 540 [35] J. Varis, J. Lepist, A simple testing-based procedure and simulation of the clinching process using finite element analysis for establishing clinching parameters, *Thin-Walled Structures* 41 (8) (2003) 691 – 709.
- [36] MatchID, www.matchidmbc.com, 2015.
- 545 [37] S. Saberi, N. Enzinger, R. Vallant, H. Cerjak, J. Hinterdorfer, R. Rauch, Influence of plastic anisotropy on the mechanical behavior of clinched joint of different coated thin steel sheets, *International Journal of Material Forming* 1 (2008) 273–276.